Title
Surface Modification with Polymers for Biomedical and Desalination Applications

Author
Curson, Paige Alexandra

Publication Date
2019

Peer reviewed|Thesis/dissertation

UNIVERSITY OF CALIFORNIA

Los Angeles

Surface Modification with Polymers for Biomedical and Desalination Applications

A thesis submitted in partial satisfaction

of the requirements for the degree of Master of Science

in Chemistry

by

Paige Alexandra Curson

2019

ABSTRACT OF THE THESIS

Surface Modification with Polymers for Biomedical and Desalination Applications

by

Paige Alexandra Curson

Master of Science in Chemistry

University of California, Los Angeles, 2019

Professor Richard B. Kaner, Chair

Hospital acquired infections lead to an increase in medical complications costing lives and billions of dollars every year. Medical implants account for the majority of these infections due to biofilm growth on implant surfaces which have proven highly difficult to eradicate with antibiotics. Here we present a preventative polymeric coating designed to easily modify biomedical surfaces, thus limiting the attachment of bacteria and growth of biofilms on these surfaces. The polymer was used to modify a number of relevant biomaterials, most notably poly-dimethyl siloxane (PDMS), showing increased hydrophilicity and thus reduced bacterial adhesion. The hydrophilic coating was durable and maintained effectiveness longer than traditional modifications such as plasma coating. Cell culture experiments confirmed that the coating resists bacterial adhesion.

In the second chapter of this thesis we introduce a novel synthesis for a triazole polymer (PTA) used for water desalination. Thin film composite membranes continue to be the leading technology for water desalination, however the current

membrane material of choice, polyamide, is extremely chlorine sensitive. Triazoles are C-H donors and thus capture chlorine. Utilizing this polymer and a new technique for membrane fabrication dubbed thin film lift off (TFLO), we created a new polymeric membrane with 1, 4 triazoles as the active layer. This polymer utilizes 1,4 triazoles which have been shown to stabilize chlorine. By incorporating these functional groups into a polymer, we fabricated a chlorine tolerant reverse osmosis membrane with a measured salt rejection of 92%.

The thesis of Paige Alexandra Curson is approved.

Xiangfeng Duan

Chong Liu

Richard B. Kaner, Committee Chair

University of California, Los Angeles

2019

Contents

Acknowledgements

Foremost, I sincerely thank my advisor Dr. Kaner for his continual support and guidance in my research. He and his lab, have truly made my research experience a memorable one.

I would like to thank and share credit for this work with the following group members: Brian Mcverry, for continued mentorship throughout both of these projects in addition to his preliminary work on the sulfobetaine polymer synthesis and TFLO work; Ethan Rao and Na He for their support in synthesis of materials as well as general guidance in experimental design and data collection; Mackenzie Anderson for the many hours spent on XPS and the development of TFLO; Alexandra Polasko for her help with bacterial adhesion data. I am so grateful to have such kind, motivational and inspirational people helping me along the way.

Finally, I would like to thank both my friends and family who have supported me on this journey. I wouldn't have gotten this far without them.

1 Characterization of Zwitterionic Polymer for Biomedical Applications

1.1 Introduction

1.1.1 Hospital Infections

It is estimated that 1 in 25 hospital inpatients get a health care associated infection known as an HAI (1). These infections are unrelated to the patients original sickness and are a serious threat to patient safety. Hospital costs for HAIs is estimated to be $28-45 billion per year and is associated with 90,000 deaths each year in the United States (2). As such, HAIs are a serious medical issue that needs to be addressed. While current methods to combat HAIs are antibiotics, due to the increase of antibiotic resistant bacteria such as MRSA, the push is for prevention rather than treatment (2). In these experiments we test a novel coating method designed to resist bacterial adhesion, the main culprit for HAIs.

The majority of the 2 million HAIs contracted each year are due to medical implant devices (3). An HAI is mainly attributed to the presence of a biofilm on the device surface. Biofilms are matrix adherent bacteria that excrete insoluble gelatinous exopolymers (4). These biofilms protect the bacteria from the hosts immune system defense mechanisms and antibiotics making them difficult to eradicate (5). Significant research has gone into the prevention of biofilms with varied success. Some coatings incorporate drugs that slowly release antibiotics or silver nanoparticles to stop the biofilm growth, however, these arent long lasting and the use of

drugs makes the antibiotic resistant problems worse. As such, we have devised a coating method that is both long lasting and non-toxic, which inhibits the growth of biofilms, thus preventing the HAIs.

1.2 Perfluorophenyl Azide Chemistry

While many polymeric coating methods already exist, they require exotic conditions such as oxygen free environments, long reaction times, or harmful chemicals. In order to have scalability, we created a copolymer that is capable of binding to relevant materials permanently under ambient conditions in a reasonable time.

Our copolymer can is broken up into two main monomers: a binding monomer, designed to have rapid reaction times and bind to a variety of substrates, and an antifouling monomer, which will prevent the formation of biofilms. In these experiments, a perfluorophenyl azide (PFPA) moiety was chosen to bind our coating to the substrate. PFPAs are highly popular due to their fast kinetics and high reaction efficiencies in order to create a scalable system (6).

The binding mechanism, as summarized in **Figure 1**, is initiated by activating the azide with 254 nm UV light. Once activated, the azide decomposes by releasing N_2, while creating a highly reactive phenyl nitrene that can form numerous covalent bonds.

The highly reactive nitrene has two main electronic statesthe singlet and the triplet states. The singlet nitrene produces either tar, Pathway I, or the more favorable covalent bonds shown in Pathway II. The singlet nitrene, under specific conditions, can also undergo inter-system crossing to form a triplet nitrene to form

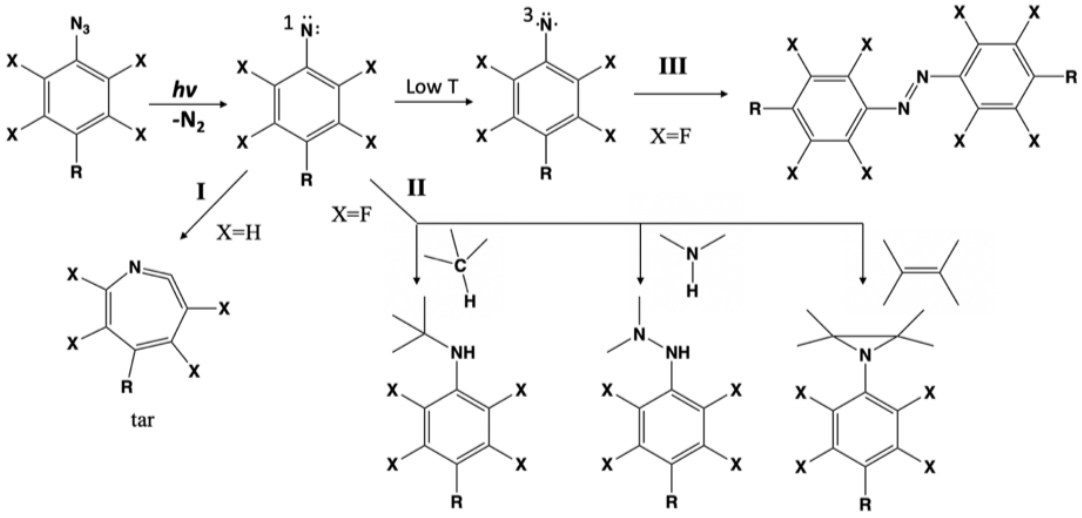

Figure 1: The azide has multiple reaction pathways once activated. Pathway I is a ring expansion when hydrogen is on the ring. Pathway II forms useful covalent bonds through addition or insertion reactions. Finally Pathway III involves intersystem crossing where the nitrene moves to a triplet state and results in a dimerization.

a dimer as shown in Pathway III. While the dimer is isolated in cryogenic matrices, it is not often seen at room temperature in appreciable amounts (7).

When X is hydrogen, as seen in Pathway I, ring expansion has an incredibly low energy barrier of only 3 kcal/mol that often results in an unusable tar (8). By adding a halogen atom, such as fluorine, shown in Pathway II, the energy barrier increases to 7.2 kcal/mol. The fluorines strong electronegative nature stabilizes the negative charge generated by the activated nitrene. This increases the yields of Pathway II, a favorable situation as it unselectively forms a wide variety of products such as CH or NH insertion and C=C addition reactions. By tailoring the reaction to favor products generated by Pathway II, PFPA can anchor our coating to a wide variety

of substrates with high yield and efficiency.

1.2.1 Sulfobetaine, an Antifouling Monomer

Using PFPA as anchoring points to our substrates, the bulk of the polymer requires antifouling capabilities to prevent infections. Fouling refers to the absorption of proteins on the substrate that directly leads to biofilm formation. While the exact mechanism of protein absorption onto substrates is not known, van der Waals forces, electrostatic interactions and hydrogen donor/acceptor bonding provide the three main contributions (9). These factors were tested by Holmlin et al. who screened a number of functional groups to determine which had the best ability to resist protein adsorption (10). They tested a variety of self-assembled monolayers with variable charges and found that ones that were electrically neutral showed the least amount of protein adsorption. This can refer to either a mixture of positively and negatively molecules or one with both positive and negative charged moieties on the same molecule. They concluded that an electrically neutral molecule lowers the contribution of electrostatic interactions, one of the main contributions to protein adsorptions. In addition to being electrically neutral, hydrophilicity and hydrogen bond donors with no acceptors were also deemed important in a potential polymer (11). The final desirable property is a non-toxic polymer so that our coating can be used in biomedical applications.

Sulfobetaine was selected as the bulk of the polymer coating due to its oxidative stability, ultra-low fouling properties, and hydrophilicity in addition to being electrically neutral. Sulfobetaine is a zwitterion meaning it has both a positive and

negative moiety and is electronically neutral. Zwitterionic materials create a unique hydration layer in comparison to other hydrophilic molecules. In more conventional hydrophilic molecules, surface hydration is due to hydrogen bonding to the surface; a zwitterionic hydration layer has much stronger electrostatic interactions with the water molecules and so the hydration layer is much thicker. This barrier helps to prevent irreversible protein absorption (12). Our final polymer, PFPA-PSB, was synthesized by copolymerizing sulfobetaine (PSB) with the PFPA monomer in an AIBN initiated reaction.

1.2.2 Polydimethylsiloxane as a substrate

While the PFPA allows the coating to bind to a variety of substrates, we focus on polydimethylsiloxane (PDMS), known as silicone, for the following experiments as it is one of many stable, biocompatible polymers used in the medical field. By modifying its surface with our coating, we are able to significantly improve its ability to reject bacterial adhesion. PDMS was chosen as it has many applications in the medical field including drug delivery implants, gas exchange membranes, and intraocular lenses (13). Its popularity stems from its low cost, ease of production, biocompatibility, and optical transparency. Unfortunately, its hydrophobic surface facilitates nonspecific protein absorption (14). In biological applications this could potentially lead to serious infections.

Previous attempts to permanently modify the surface of PDMS have been unsuccessful. Plasma treatment is commonly used to modify PDMSs surface by increasing the number of surface silanol bonds, thus increasing hydrophilicity of the surface.

Unfortunately plasma treatment is not particularly scalable, limiting it to laboratory uses. In addition to scalability issues, plasma treatment is not a long-term surface modification. Plasma oxidation can be readily reversed in as little as 15 minutes due to thermodynamic instability. This process dubbed hydrophobic recovery is due to the low glass transition temperature of PDMS (-120°C), where the chains are highly mobile and so any hydrophilic surface modification is rapidly hidden by the bulk in order to minimize the surface energy (15). Hydrophilic recovery can also be caused from chains of low molecular weight, stemming from uncross-linked PDMS or residual crosslinking agent, which can more easily move to the surface. One method to combat this is thermal aging, which lowers the number of these chains, thus increasing the time the surface stays hydrophilic. This method, however, is still not permanent and is time consuming as hydrophobic recovery will still occur within a few days (16). PDMS treatments with other polymers such as the coating synthesized by Sung et al. (17) in an attempt to create a more permanent surface modification still rely on this silanization pretreatment. These methods clearly show a need for hydrophilic modification of PDMS that is scalable and long lasting. Because we have multiple binding sites along our polymer when we activate it on our surface, it will become heavily crosslinked. We later show that this crosslinking prevents hydrophobic recovery.

1.2.3 Surface Energy Calculations

Wettability is one of the most influential parameters affecting protein absorption on a surface with hydrophobic surfaces tending to have more adsorption than hy-

drophilic ones (18). Surface free energy measurements are one way to quantify the hydrophilicity of the modified surface.

Surface free energy is defined as the work necessary to increase the surface area of the solid phase. It is directly related to wettability as when a liquid and solid forms an interface, they strive to reduce the free energy, which results in a particular shape on the surface. Wettability is directly measured by the contact angle as seen in **Figure 2**. The contact angle is the balance between the liquid adhesive forces between the surface and cohesive forces within itself. The smaller the surface tension, i.e. the cohesive force, the smaller the contact angle as the liquid will spread. **Figure 2** shows the relationship between contact angle and the surface tension of the liquid, solid and the interface.

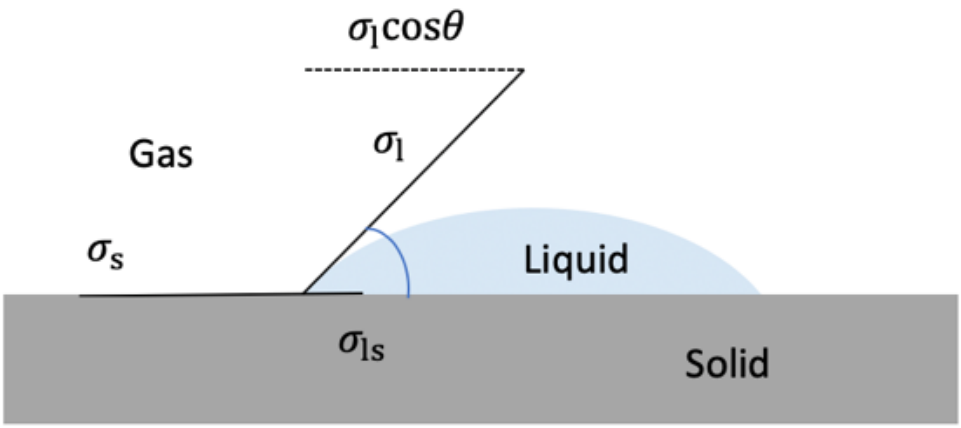

Figure 2: This figure shows the contact angle as the angle between the baseline and the curvature of the droplet.

Thomas Young described the relationship between the contact angle θ , the sur-

face free energy of a solid σ_s, the surface tension of the liquid σ_l, and the interfacial tension between the liquid and the solid σ_{sl} in **Equation 1** (19).

$$\sigma_s = \sigma_{sl} + \sigma_l * cos\theta \tag{1}$$

However, this is for an ideal surface and the interfacial tension, σ_{sl}, and the surface free energy of the solid, σs, are both unknown. Many scientists have come forward with their own ways of calculating surface free energy during the last 50 years. The Fowkes method proposes that the surface free energy of a system can be separated into two main components, dispersive (σ^d) and polar (σ^p) with the sum of the two parts equaling the total surface energy as described in **Equation 2** (20):

$$\sigma = \sigma^d + \sigma^p \tag{2}$$

The dispersive part is calculated using the contact angle of one purely dispersive liquid and the polar part is determined using a different liquid with polar parts. The two liquids traditionally used for these calculations are water for the polar portion and diiodomethane for the dispersive part. As each liquid has a different interaction with the solid, their contact angles would differ respectively. For example, a more polar solid would be more similar to water, having better adhesion and thus a smaller contact angle. In this way, by dividing the surface free energy into two parts, we can better characterize the type of solid.

While Fowkes did the first work on calculating surface free energy, many others have tailored the calculations to obtain more reliable results. We used the Wu method

to calculate surface free energy, which is most often used for polymers (21). This method utilizes a series of nonlinear **Equations (3)** and **(4)** in order to solve for both the polar and dispersive components.

$$(b_1 + c_1 - a_1)\sigma^d\sigma^p + c_1(b_1 - a_1)\sigma^d + b_1(c_1 - a_1)\sigma^p - a_1b_1c_1 = 0 \quad (3)$$

$$(b_2 + c_2 - a_2)\sigma^d\sigma^p + c_2(b_2 - a_2)\sigma^d + b_2(c_2 - a_2)\sigma^p - a_2b_2c_2 = 0 \quad (4)$$

With $a_n = (1/4)\sigma_n(1 + cos\theta_n)$, $b_n = \sigma_1^d$, and $c_n = \sigma_n^p$ (n=1 or 2); σ_1 = the contact angle of water and σ_2 = the contact angle of diiodomethane. $\sigma_1 = 72.8$ dynes/cm, $\sigma_1^d = 22.1$ dynes/cm, $\sigma_1^p = 50.7$ dynes/cm, $\sigma_2 = 50.8$ dynes/cm, $\sigma_2^d = 44.1$ dynes/cm, $\sigma_2^p = 6.7$ dynes/cm. By solving for the dispersive and the polar components separately we then use **Equation 2** to calculate the total surface free energy.

1.3 Materials and Methods

4-Azidotetrafluorobenzoic Acid: pentafluorobenzaldehyde was combined with 1.3 molar equivalents of sodium azide in a 2:1 ratio of acetone to water. The solution was refluxed overnight and extracted in water:diethyl ether before the solvent was removed using a rotary evaporator. 0.586 g of the powder was added in 0.8 mL of 20% aqueous NaOH in 10 mL methanol and 1 mL of water. The solution was stirred overnight at 25 °C. 2 M HCl was then added until the solution reached a pH < 1 and the product was extracted using chloroform:water. Once purified, the product was once again added to a methanol: aqueous NaOH mixture (2:1) until the

product dissolved.

UV-Vis: UV/vis spectra of PFPA-PSB was taken in water using a Hewlett Packard 8453 UV-vis spectrophotometer. For the second spectra, 4-azidotetrafluorobenzoic acid was added to a 1:1 ratio of 20% aqueous NaOH and MeOH in order to deprotonate the molecule before it was measured.

Coating PDMA substrates with PSB: PDMS substrates were prepared by mixing a 10:1 ratio of elastomer: curing agent (Syglard 184), followed by curing at 80 °C for 1 hour. Researchers cut PDMS sheets into 3 mm diameter disks. A PSB coating solution (2 mL) with a concentration of 2, 5, or 10 mg mL-1 was placed and spread out on the surface of each disk, followed s by exposure to 254 nm UV light for 10 minutes, rinsing with deionized, and drying with air.

Contact angle visualization and measurements: Water contact angle on various substrates, such as PDMS, nylon 66, polystyrene, polyvinyl chloride, and polyethylene was measured by placing 17 μL of deionized water on the flat substrates at room temperature followed by imaging them. The images were analyzed using the FTA32 version 2.1 software to measure the contact angles. To study the hydrophobic recovery of water contact angles on PDMS, the substrates were divided into two groups: (i) uncoated PDMS sheets, which were treated using O2 plasma (Plasma Etch PE25-JW Plasma Cleaner, NV, US) for 1 min, and (ii) PDMS sheets that were coated with PSB with a concentration of mg mL-1. After modification, water contact angle was measured after 1, 2, 4, 7, and 10 days.

X-ray photoelectron spectroscopy (XPS): A Kratos AXIS Ultra DLD with a monochromatic Al K X-ray source operated at 10 mA and 15 kV was used to perform

XPS measurements. Individual high-resolution spectra and survey spectra were collected using 20 and 160 eV pass energies, respectively. Data processing were carried out using CasaXPS 2.3 software. The spectra were calibrated using binding energies by realizing the hydrocarbon peak in the C 1s high-resolution spectra at 284.6 eV.

Cell adhesion: Trypsinized fibroblasts cells were seeded on PSB-coated 96-well plates by placing 100 μL of the cell suspension (cell density 1 105 in 1 mL media) on the treated well plates, followed by culturing for 24 hour. Uncoated well plates were used as a control.

Live/dead assay: To assess the cell viability, a live/dead fluorescence assay was used. The staining solution was prepared by adding ethidium homodimer-1 (20 μL) and calcein AM (5 μL) to DPBS (10 mL). To perform the assay, the cells were incubated with 1 mL of the staining solution for approximately 20 min and imaged using a fluorescent microscope (Axio Observer 5, Zeiss, Germany) at excitation/emission wavelengths 494/515 nm for calcein and 528/617 nm for ethidium homodimer-1.

1.4 Results and Discussion

1.4.1 UV-Vis

Before coating substrates UV-Vis spectra were taken of the PFPA-PSB polymer solution to determine if the azide was activated and to be able to speculate as to the mechanism taking place.

A 10 mg/mL solution of PFPA-PSB polymer was prepared and illuminated at 254 nm for 30 minutes. The resulting solution turned a pale yellow as seen in **Figure 3**. UV-vis spectra were measured to determine the cause of this color change.

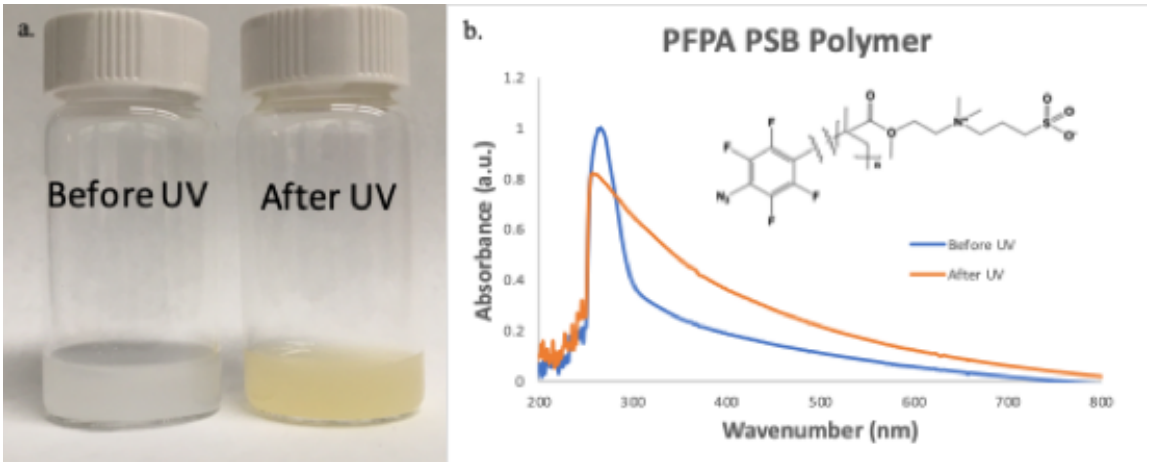

Figure 3: (a) Polymer solution before and after UV irradiation. (b) UV-Vis spectra of the PFPA-PSB polymer.

Before UV irradiation, there is a distinct absorption peak at 267 nm, which is common for azide compounds. The peak, however, is broad showing that the polymer probably has other electronic states absorbing UV radiationas this conjugated polymer has multiple double bonds along its backbone. After irradiation, the peak height lessens, while also noticeably broadening. After azide activation, the most likely mechanism is for a singlet nitrene to form, subsequently crosslinking along the backbone of the PSB polymer. The broadening of the peak shows that there are more electronic states absorbing UV radiation. The broad portion also seems to be more pronounced compared to before UV irradiation, which suggests that there are enhanced effects from the conjugated backbone. The yellow color could then be due to the azide binding close to the double bonds along the PSB, changing their energy states. Looking back at **Figure 3**, there is a second possible mechanism the creation of a dimer through intersystem crossing and a triplet nitrene. In this pathway, the

triplet nitrene binds to a second triplet nitrene rather than the surface or along the backbone of the polymer.

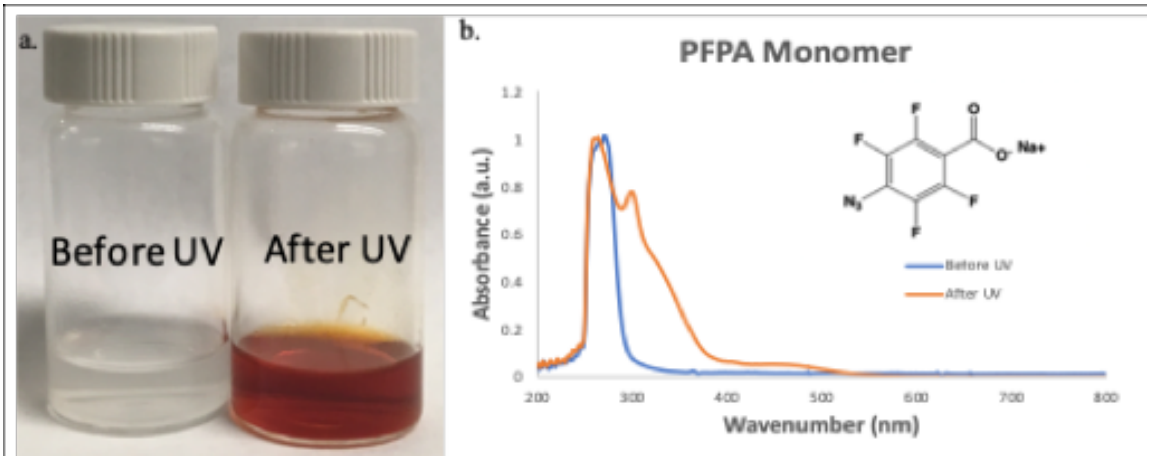

Figure 4: (a) Monomer solution before and after UV irradiation. (b) UV-Vis spectra of the monomer.

To test this theory a PFPA monomer, 4 azido tetrafluorobenzoic acid, was synthesized and purposefully dimerized. A 5 mg/ml solution of this benzoic acid in 20% aqueous NaOH/ methanol was used in order to deprotonate it. Methanol catalyzes the intersystem crossing by lowering the energy gap between singlet and triplet nitrene, resulting in more triplet nitrene being produced (7). The product was illuminated under 254 UV light for 20 minutes and can be seen in **Figure 4a**. A dramatic color change compared to the un-irradiated polymer is observed, as this compound is highly absorbent in the visible region. Before UV irradiation, there is a strong peak once again at 267 nm; however, compared to the polymer, the monomers peak is much narrower. This further indicates that the broadness in the polymers peaks is likely due to the influence of the PSB and not the PFPA. After UV irradiation, a second peak forms at 300 nm in addition to the peak at 267 nm.

The 300 nm peak is clearly caused by the triplet nitrene forming the dimerization. However, this does not prove that the color change seen from activating the polymer is from the dimerization. The peaks from the monomer are much narrower than the polymer and so we can conclude that the broadness seen in **Figure 2b** is due to the PFPA binding along the backbone of the PFPA. When comparing UV-Vis spectra it is very unlikely that the polymer is forming a dimerization and the yellow color is purely caused by changes in the energy states near the double bonds. Since the polymer readily binds along its backbone, it will lead to a much more heavily crosslinked surface. which will likely stop hydrophobic recovery.

1.4.2 XPS

XPS was utilized to determine if the PFPA-PSB covalently binds to PDMS. The data seen in **Figure 5a** indicate that the PFPA-PSB coating did successfully bind to the PDMS. Sulfur peaks from the XPS are seen on the modified surface compared to the control; however, the biggest indication of binding is through the N 1s peak. If the polymer was only physically coating the surface, 3 different nitrogen species corresponding to the azide would be seen. However, only one peak at about 400 eV is seen from the N 1s peak. This signifies that the azide forms covalent bonds with the polydimethylsiloxane through CH insertion as shown in **Figure 5b**.

1.4.3 Surface Free Energy and Contact Angle

To test the hydrophilicity of the surface modification, contact angles were measured. The contact angle of both water and diiodomethane were used to calculate the surface

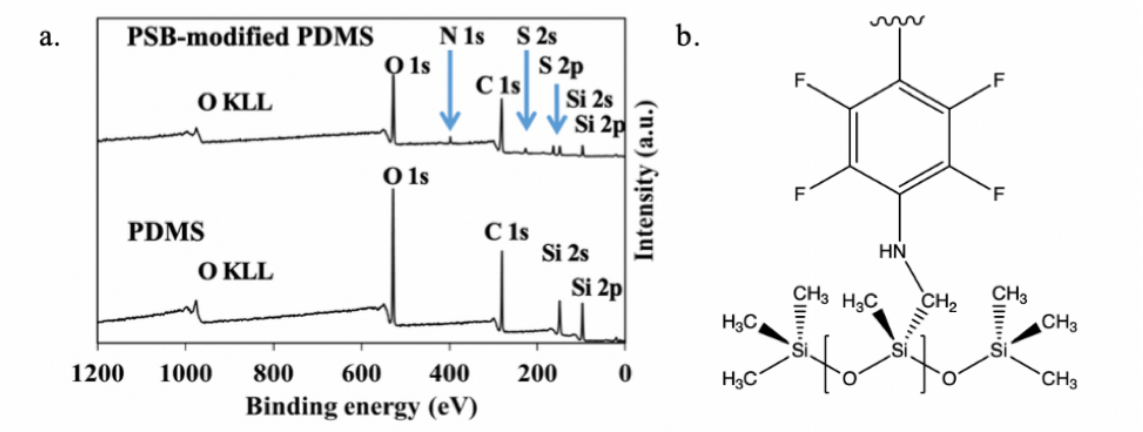

Figure 5: (a)XPS spectra of PDMS with (top) and without (bottom) the PFPA-PSB coating. (b) Expected bond formed after modification.

energy of both the unmodified and modified PDMS surface using the Wu method. The values are summarized in **Table 1**.

Substrate	Water θ	Diiodomethane θ	γ^p (dynes/cm)	γ^d (dynes/cm)	γ (dynes/cm)
Control PDMS	107.5°	66.56°	29.99	0.02	30.01
Modified PDMS	22.0°	38.31°	27.37	41.57	69.14

The water contact angle was significantly smaller on the modified PDMS at 22.0° compared to 107.5° showing that the surface became super-hydrophilic. While the diiodomethane contact angle also decreased after modification, the difference was much less significant. Interestingly, the contact angle for diiodomethane was larger than the water contact angle on the modified PDMS.

The total surface free energy of the modified PDMS was more than twice the

unmodified sample.

Contact angle was also used to test our coatings ability to withstand PDMS innate ability for hydrophobic recovery. The covalent bonds to our substrate in addition to the substantial crosslinking between other PFPA-PSB chains lead us to believe it will not undergo hydrophobic recovery as readily as plasma treatment. To test this, the contact angle was measured every two days over a 10-day period comparing the two different coating methods. **Figure 6** shows the contact angle changing over time between plasma treated PDMS and our PSB-coated PDMS. While both coatings started off at about 10°, the plasma coating quickly degrades resulting in an eventual contact angle of about 80°, close to uncoated PDMS. However, the PSB-coated PDMS is still around 25° at the end of the 10-day period. It is clear that the PSB-coated PDMS resists hydrophobic recovery and maintains its super-hydrophilic surface over time relative to the plasma coating. This ability to resist hydrophobic recovery is one of the most important aspects of our coatings ability to be useful in clinical applications as the surfaces dont appear to degrade over time.

Contact angle measurements were again used to study the ability for the PSB-coating to bind to a variety of clinically relevant substrates. **Figure 7** compares the contact angle between PDMS, nylon 66, polystyrene, polyvinyl chloride, and polyethylene showing that all substrates were successfully modified compared to the unmodified ones. All modified substrates demonstrated contact angles of ¡20°, while the unmodified ones were ¿60°. This clearly shows the versatility of the azide chemistry and its ability to bind to a variety of substrates.

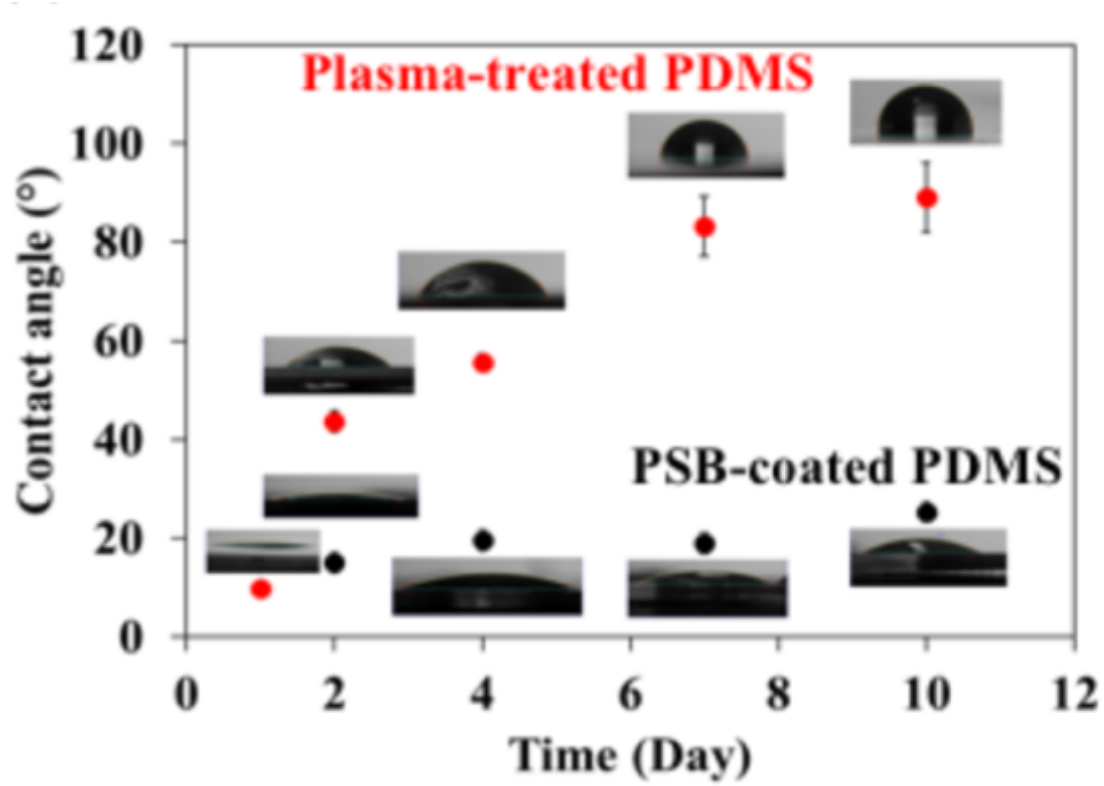

Figure 6: Contact angles were taken over the span of 10 days for both PFPA-PSB modified PDMS and plasma modified PDMS.

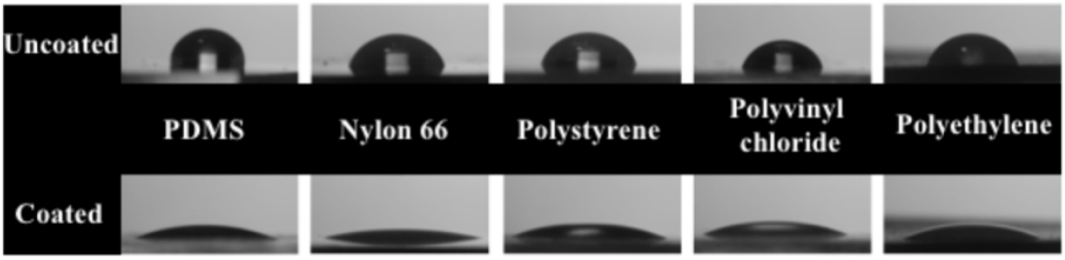

Figure 7: Contact angles were taken of a variety of substrates: PDMS, Nylon 66, Polystyrene, Polyvinyl chloride, and Polyethylene.

1.4.4 Bacterial Adhesion

Since bacterial adhesion is the prerequisite to biofilm formation, to fully test whether or not the PFPA-PSB coating will resist bacterial adhesion, a 24-hour fibroblast cell culture and live/dead staining was performed to show how the coating compared to unmodified PDMS. These data are shown in **Figure 8a**.

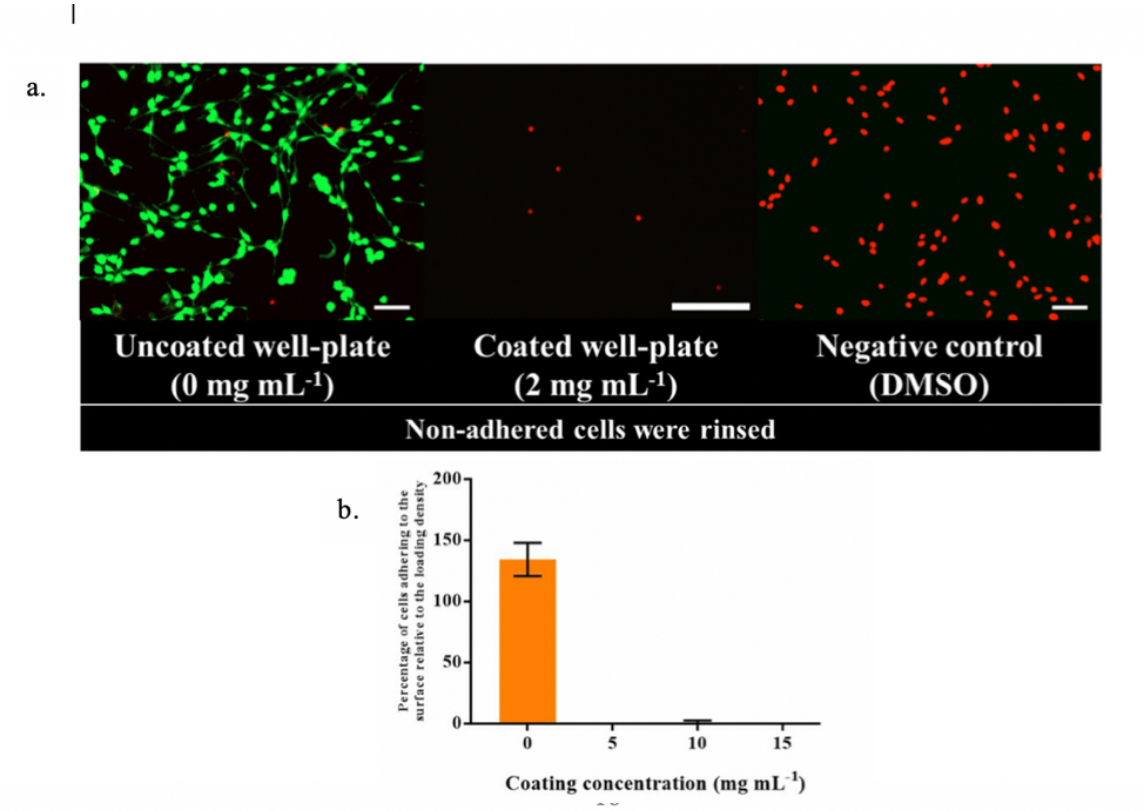

Figure 8: (a) Live/dead staining of fibroblast cells after a 24 hour culture on both an unmodified and modified substrate. (b) Shows the percentage of cells adhering to the substrates

The green stain represents live cells, while the red stain represents dead cells. The uncoated PDMS (on the left) was covered in living cells as once an initial biofilm

was created, the cells reproduced, covering the entire surface. The PFPA-PSB coated plate, on the other hand, showed no live cells and very few dead ones. Since there was no adhesion and ability to grow and reproduce, the few cells that did adhere died. The negative control showed that all of the adhered cells died in DMSO. **Figure 8b** compares the percentage of cells adhering to the surface between the uncoated and coated PDMS. The uncoated PDMS had over 100% cell adhesion showing the reproduction of cells over the 24-hr period. The coated PDMS had almost no cell adhesion on the surface.

1.5 Conclusion

We have shown through a variety of characterization techniques that the PFPA-PSB successfully binds to a number of substrates, most notably polydimethylsiloxane (PDMS). Using XPS, we were able to show that covalent bonds formed between the PFPA moiety and PDMS with fast kinetics under ambient conditions. UV-Vis indicated that activation of PFPA forms a thickly crosslinked layer on the surface. We believe that this crosslinking is what prevents hydrophobic recovery, which was not seen after measuring contact angles for a week. Having a robust surface coating that is long-lasting is important for biomedical applications. Surface free energy calculations demonstrated that the surface energy substantially increased after modification. This increase in energy also corresponds to a substantial decrease in bacterial adhesion as a thin water layer essentially precludes live bacteria from growing on the coated substrate after 24 hours.

1.6 Future Work

While our PFPA-PSB polymer has shown excellent antifouling capability in the lab, real life protein absorption is much more complicated as the influence among different proteins and biological environments can have a profound impact on protein absorption (22). Bacterial adhesion experiments with a mixture of proteins and eventually clinical trials will need to be carried out to fully understand the impact of the PFPA-PSB coatings on medical devices.

Another interesting test would be to see how polymer chain length affects antifouling properties. Longer polymer chains have an added steric repulsion to proteins likely increasing their antifouling properties (22). While preliminary testing was carried out with a PFPA sulfobetaine small molecule that was relatively hydrophobic, therefore bacterial adhesion studies were not performed. By changing the reaction time or the AIBN concentration, we can tailor the polymer length to find the ideal size for biomedical applications.

1.7 References

1. Health Care-Associated Infections. *Health.gov*, Office of Disease Prevention and Health Promotion, health.gov/hcq/prevent-hai.asp.

2. P.W. Stone, *Expert Rev Pharmacoecon Outcomes Res.*. **2009**, 9, 417422.

3. R.P. Wenzel, *Clin. Infect. Dis.*. **2007**, 15, 45.

4. J.D. Bryers, *Biotechnol. Bioeng.*. **2008**, 100, 1-17.

5. P. Herman-Bausier, Y.F. Dufrene, *Science*. **2018**, 359, 1464-1465.

6. L. Liu, M. Yan, *Acc. Chem. Res.*. **2010**, 43, 1434-1443.

7. R. Poe, J. Grayzar, M.J. Young, E. Leyva, K.A. Schnapp, M.S. Platz, *J. Am. Chem. Soc.*. **1991**, 113, 3209-3211.

8. R. Poe, K.A. Schnapp, M.J. Young, J. Grayzar, M.S. Platz, *J. Am. Chem. Soc.*. **1992**, 114, 5054-5067.

9. M.G. Cacace, E.M. Landau, J.J.Q. Ramsden, *Rev. Biophys.*. **1997**, 30, 241-277.

10. R. Erik Holmlin, X. Chen, R. G. Chapman, S. Takayama, and G. M. Whitesides. *Lang.*. **2001**, 17, 2841- 2850.

11. E. Ostuni, R.G. Chapman, R. E. Holmlin, S. Takayama, G.M. Whitesides, *Lang.*. **2001**, 17, 5605-5620.

12. H. Zhang, M. Chiao, *J. Med. Biol. Eng.*. **2015**, 35, 143.

13. *Natural and Synthetic Biomedical Polymers*, (Eds. S.G. Kumbar, C.T. Laurencin, M. Deng), Amsterdam, Netherlands, **2014**.

14. A. Gokaltun, M.L. Yarmush, A. Asatekin, O.B. Usta, Technol. Singap. *World Sci.*. **2017**, 5, 1-12.

15. G.G. Bausch, J.L. Stasser, J.S. Tonge, M.J. Owen1, *Plasmas Polym.*. **1998**, 3, 23.

16. D.T. Eddington, J.P. Puccinelli, D. J. Beebe, *Sens. Actuators, B.* **2006**, 114, 170-172.

17. W.C. Sung, H.H. Chen, H. Makamba, S.H. Chen, *Anal. Chem.* **2009**, 81, 79677973.

18. C.P. Stallard, K.A. McDonnell, O.D. Onayemi, J.P. OGara, D.P. Dowling, *Biointerphases.* **2012**, 7.

19. T. Young, *Royal Soc.*. **1805**, 19.

20. F.M. Fowkes, *Ind. Eng. Chem.*. **1964**, 56, 40-52

21. S. Wu, *J. Polymer. Sci.*. **1971**, 34, 19-30.

22. H. Zhang, M. Chiao, *J. Med. Biol. Eng.*. **2015**, 35, 143.

2 Novel Triazole Used for Desalination

2.1 Introduction

2.1.1 Reverse Osmosis Membranes

Reverse osmosis is currently the most popular desalination technology, as it has a low energy cost and achieves extremely high salt rejection (1). Because this method has almost completely reached its theoretical potential for energy efficiency, few improvements have been made in recent years. However, reverse osmosis membranes must not only have high rejection rates, but should be chlorine tolerant, and demonstrate resistance to fouling. These qualities have been difficult to achieve using current membrane fabrication techniques. In these experiments, we introduce the ability to fabricate a novel polymeric membrane that has demonstrated high salt rejection with the possibility of being chlorine tolerant.

Early reverse osmosis membranes were made from cellulose acetate in a symmetrical membrane. These membranes achieved high salt rejection, however, their permeability was quite low, so they were not scalable (2). Years later, Loeb et al. created an asymmetric membrane using cellulose acetate that was composed of an ultra-thin dense layer on top of a microporous support (3). While the salt rejection this method yielded was similar to its symmetrical counterpart, its flux was over 200 times greater than the symmetric membrane. The success of this membrane confirmed that the effective thickness of membranes can be much smaller than the total membrane thickness.

Cellulose acetate continued to be popular in membrane experiments, but it has

significant drawbacks. These membranes are limited to water with fairly low salinity, and they are susceptible to hydrolysis with changing pH (4,5). A sturdier polymer that can be used in a wider range of applications is therefore needed. Strathmann and Michaels screened a number of polymers to determine which properties optimize both water permeability and salt rejection (6). They found a strong correlation between high water sorption and higher permeabilities, as shown in **Figure 1**.

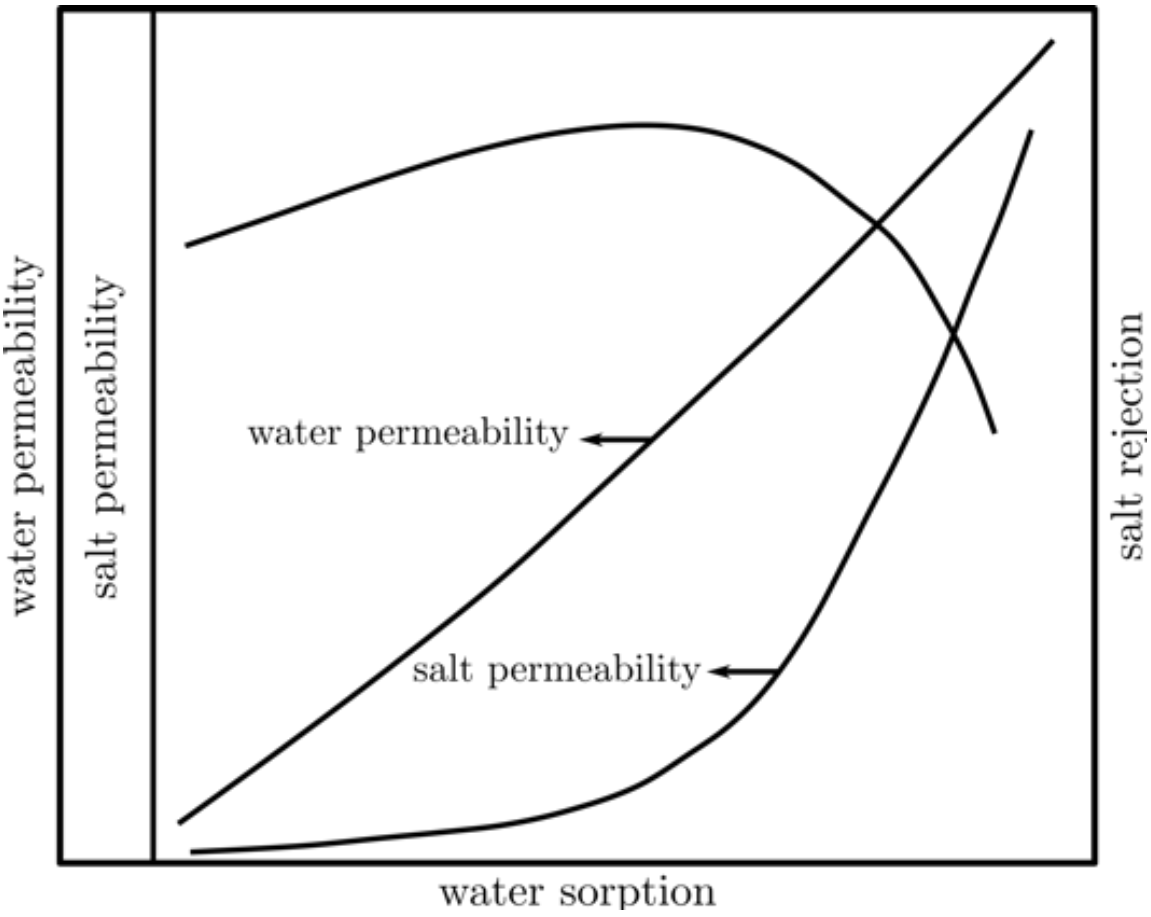

Figure 1: Water and salt permeabilities as a function of the water sorption and salt rejection levels (6)

They also found that the distribution of water within the membrane impacted permeability and water rejection. If the water clusters, as is thermodynamically preferred, much more energy is required for it to permeate through the membrane. Strathmann and Michaels concluded that the best polymers for salt rejection via reverse osmosis needed to possess a high glass transition temperature. These polymers have a rigid backbone thus undergoing minimal chain rearrangement, which prevents water molecule clustering. If a polymer is linear, it can rearrange itself to accommodate water clusters. One polymer in particular that demonstrates both high rejection as well as high permeability is polyamide. However, polyamide films are highly susceptible to damage from chlorine, which is a popular chemical additive in water treatment processes. This problem highlights the need for a chlorine-tolerant membrane with good salt rejection.

2.1.2 Chlorine Tolerance

A new generation of polyamide-based membranes have much higher salt rejection compared to traditional cellulose acetate membranes, but they tend to react poorly with chlorine. During the desalination process, chlorine is often used as a disinfectant as well as an oxidizer to remove certain metals. Therefore the chlorine must be completely removed to protect the integrity of the membrane. Research shows that chlorine permanently destroys polyamide membranes due to polymer cleaving, thus reducing the molecular weight. This polymer degradation decreases the tightness of the membrane, which allows more salt to flow through. **Figure 2** shows the process that occurs when hypochlorite (chlorine bleach) is introduced into the feed water

(7). Chlorine is stabilized on the amide due to the electron-withdrawing effect of the carbonyl (4). The aromatic ring is then vulnerable to electrophilic substitution, allowing the chlorine to readily attack the ring. Once the ring is destroyed the chlorine can once again add onto the amide. This reaction mechanism ultimately results in the polymer being cleaved at the amide bond. Afterwards, Hoffman rearrangement creates the quinone structure (8).

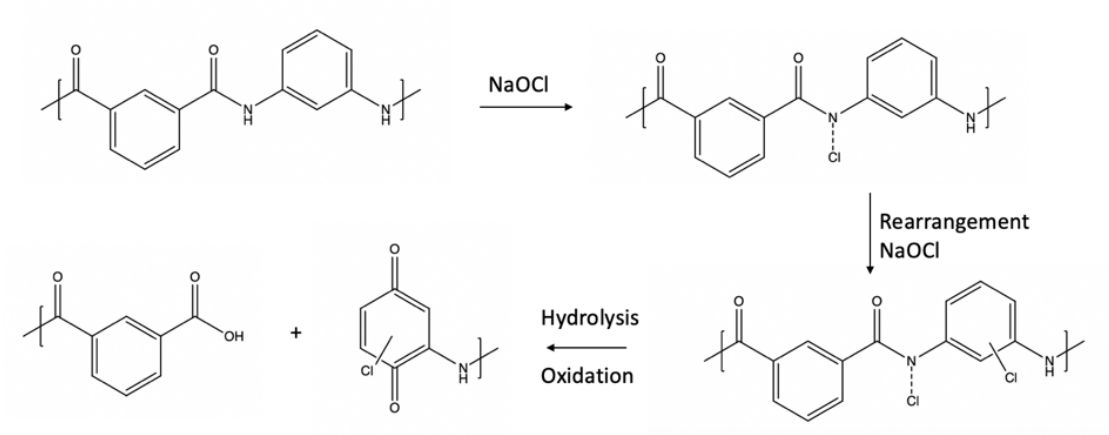

Figure 2: Breakdown of polyamide when introduced to chlorine bleach.

Researchers have subsequently added a methyl group to the amide, making it less reactive, thus protecting the polyamide from chlorination (4). Unfortunately, these strategies have also shown negative effects regarding salt rejection. A membrane that features both high salt rejection and chlorine tolerance requires using a different polymer for the active layer.

In our membrane, we used a polymer with a synthetic receptor for chlorine to trap the chlorine ions on the membrane. However, because chlorine is relatively small, high membrane selectivity is needed. Recently, Liu et al. created a small molecule

binding cage using CH donors to attract the chlorine (9). 1, 2, 3 triazoles have been shown to be strong hydrogen bond donors due to the nitrogens in the ring, which have strong electron-withdrawing effects on the remaining free carbon atoms (10). Chlorine has also been shown to be a strong hydrogen bond acceptor (11). This process is visually demonstrated in **Figure 3**.

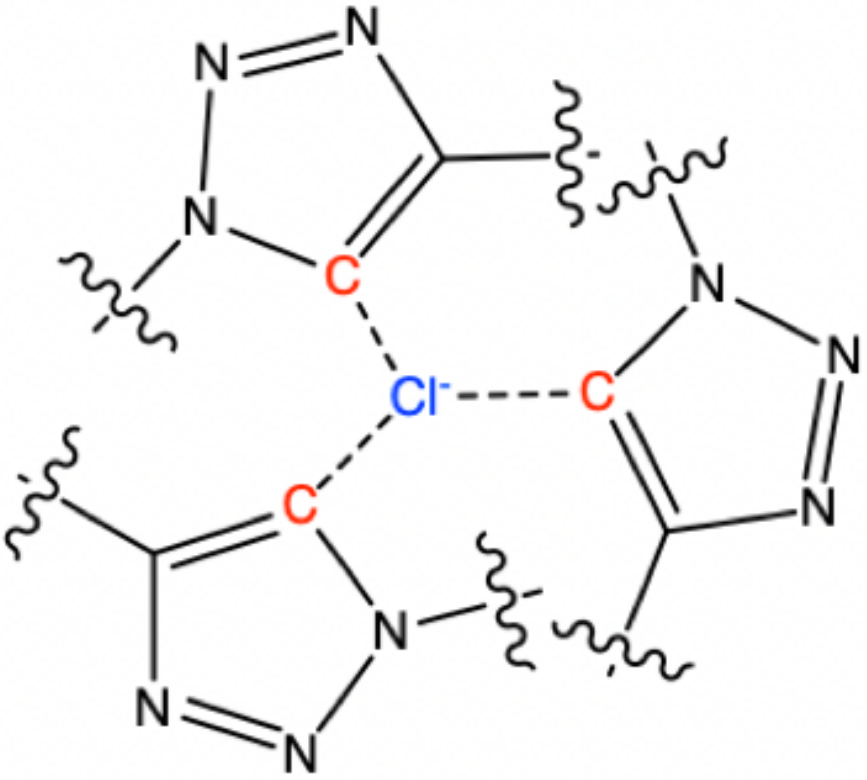

Figure 3: Chlorine capture utilizing 1,4 triazoles.

While these triazoles show high affinity for chlorine, incorporating a rigid structure can also increase chlorine capture (11). Rather than using small molecules, we synthesized a polymer using 1, 2, 3 triazoles alternating with aromatic groups to create a fairly rigid system large enough to encompass chlorine atoms.

2.1.3 Click Chemistry

We used click chemistry to create the triazoles in our polymer. Click chemistry defines a variety of reactions that fit an exact criteria: simple reaction conditions, simple product isolation, high yields and stereospecificity (12). These reactions are thermodynamically driven, with a driving force of around 20 kcal/mol (12). This causes a rapid reaction with a highly selective product. While these conditions can define a number of reactions, we use the cycloaddition of azide and alkyne. A generic scheme is shown below in **Figure 4**.

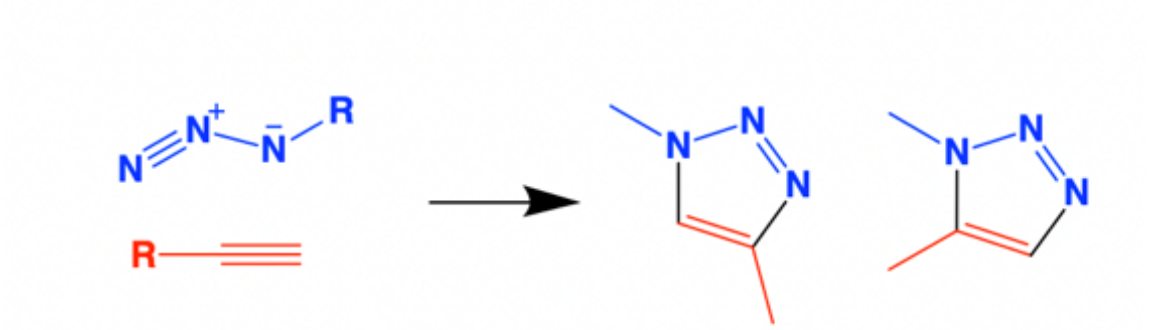

Figure 4: Generic click chemistry reaction scheme using azides and alkynes to create triazoles.

This reaction can be demonstrated in water simply by using heat. However, the reaction is not very selective and produces both the 1,4 and 1,5 disubstituted

triazoles. Copper (I) is used as a catalyst to selectively produce 1,4 disubstituted triazoles (13). While the copper can be reused and can be removed from the reaction, copper residue can impact later salt rejection.

In these experiments, we use an activated perfluorophenyl azide and propargylamine, a simple alkyne. The electron-withdrawing abilities of the fluorine facilitate a metal-free click polymerization (14). Without the copper catalyst, the reaction is environmentally friendly and allows for easy cleaning of the product. Metal-free click polymerizations have also been found to be regioselective, with 92% 1,4 disubstituted triazoles being produced in dimethylformamide (DMF) with high efficiency (15). A simplified version of the synthesis is shown in **Figure 5**.

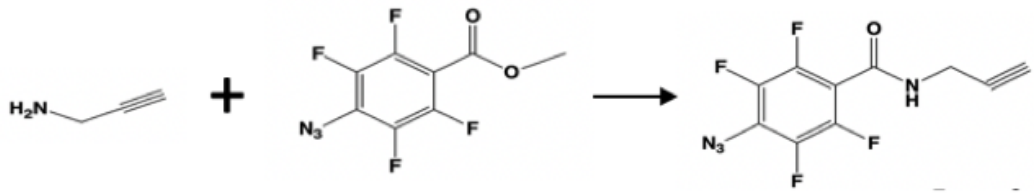

Figure 5: Brief synthesis showing the combination of the azide and the alkyne on the same molecule will create a polymer.

By functionalizing two sides of the monomer, polymerization with itself is simplified. As a result, only a solvent and heat are needed for the polymerization. While this polymer should be chlorine tolerant and exhibit high salt rejection, developing a membrane with this as an active layer continues to be challenging.

2.1.4 Thin Film Lift Off (T-FLO

To create reverse osmosis membranes, polyamide is grown on polysulfone supports through a polycondensation reaction (16). This interfacial polymerization limits the number of materials that can be integrated into the membrane. McVerry, Anderson et al. have developed a novel technique called Thin-film lift off (T-FLO) (17). This technique involves casting the active layer separately from the support, which increases the range of materials that can be fabricated. The active layer is cast on a clean glass substrate using a doctor blade and cured overnight. An epoxy is used as the support because it has a tailorable pore size and it interacts well with the active layer by forming strong covalent bonds. **Figure 6** visually demonstrates the procedure for creating the membrane.

For this process, the active layer must have functional groups that can form covalent bonds with the epoxy. Polyimides, polyimidizoles and amines were all found to react with the epoxy, so the active layers used had amines throughout the epoxy. Using this technique, we were successful in creating a membrane with a polytriazole (PTA) active layer.

2.2 Experimental

2.2.1 Polymer Synthesis

Methyl 4-azidotetrafluorobenzoate was synthesized by refluxing 9.8 g of methyl pentafluorobenzoate and 3.4 g (1.2 equivalents) of sodium azide in 90 mL of a 2:1 water: acetone mixture overnight. The resulting solution was then purified by separation

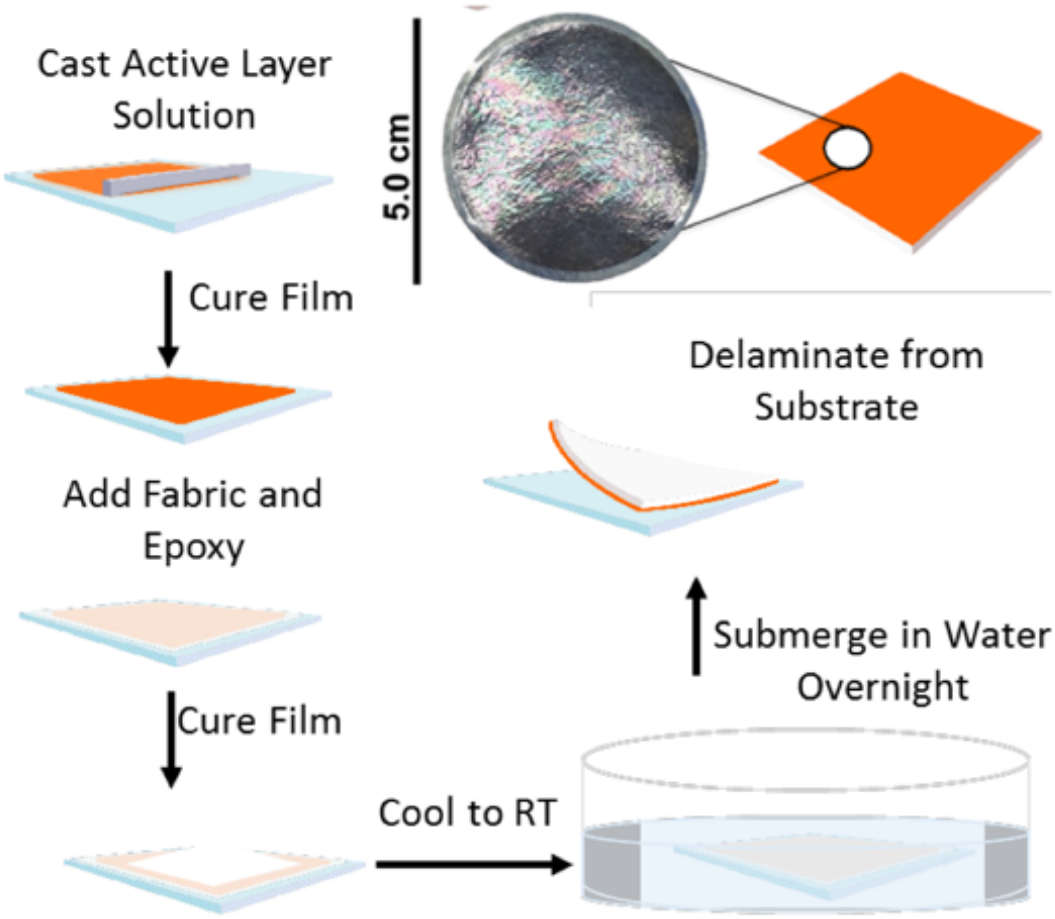

Figure 6: The TFLO is a membrane fabrication process. It involves the casting of the active layer first before adding the epoxy support.

in diethyl ether and water. Fluorine NMR in deuterated chloroform was used to confirm the azidation was successful.

4- Azidotetrafluorobenzoic Acid: To remove the methyl group and deprotect the molecule, methyl 4-azidotetrafluorobenzoate (5 grams) was added to a solution of 20% aqueous NaOH (80 mL) in MeOH (100 mL) and water (10 mL), and stirred overnight at room temperature. 2.0 M HCl was then added until the resulting pH

was <1. Chloroform and water were used to extract the final product, which was a colorless solid. Proton and fluorine NMR were again used to show the success of the reaction in deuterated chloroform.

N-Succinimidyl 4-Azidotetrafluorobenzoate: 4- Azidotetrafluorobenzoic acid, N-hydroxysuccinimide (NHS), and dicyclohexylcarbodiimide (DCC), all at one equivalent were added to dichloromethane at approximately 0.15 M. The mixture was stirred at room temperature overnight and covered, but with a needle to release gas. The mixture was filtered and the filtrate evaporated to a pale yellow color. The solid was recrystallized in a chloroform/hexane solution to remove excess DCC and NHS, leaving a white solid.

4- Azidotetrafluorobenzoate propargylamide: Equal amounts of the n-succinimidyl 4-azidotetrafluorobenzoate was added to chloroform (0.057 M) and stirred overnight at room temperature. The resulting solution was separated in chloroform and water and left as a pale brown solid.

Poly-triazole (PTA) - 2.7 mmol of 4-azidotetrafluorobenzoate propargylamide was added to 3.375 mL of DMF and stirred for 2 days at 100 °C. The resulting polymer was extremely viscous and dark brown in color. The resultant solution was diluted with 20 mL chloroform and added dropwise to 1.0 L of hexane-chloroform (10:1 by volume). The precipitates stood overnight and were subsequently filtered and washed with hexane leaving behind a brown solid. NMR and IR were used to track the progress of the polymerization.

2.2.2 Membrane Casting

The active layer was a 2:1 ratio of a commercial solution of celazole polybenzimidazole (Performance Products Inc.), (PBI), 10% in dimethylacetamide (DMAc) added to the poly-triazole PTA. The addition of the PBI created a sturdier membrane with easier liftoff. The active layer was cast onto a clean glass substrate using a doctor blade. The film was baked in the oven at 80 C overnight to ensure that all of the solvent had evaporated. The support layer was a mixture of 3.25 g polyethylene glycol (a 1:1 mixture of PEG-200 and PEG-400), 440 mg 4,4-methylenebis(cyclohexylamine), and 1.25 g of Bisphenol A diglycidyl ether (Sigma-Aldrich). The mixture was stirred for 3 hours before it was poured on top of a woven glass fiber cut to 11 cm by 14 cm on top of the active layer. The membrane was then baked at 120 °C for 3 hours before it was put into a water bath overnight. The membrane easily pulled off from the glass substrate with no apparent defects to the active layer.

2.2.3 Salt Rejection Testing

A 300 mL dead end cell apparatus was used to test the membranes salt rejection capabilities. Five centimeter coupons were punched out of flat sheets and loaded into the apparatus. 200 mL of 2,000 ppm NaCl were used for rejection testing. The dead end cell was operated at 800 psi overnight and the permeate was collected. The rejection was calculated by testing the conductivity of the permeate and comparing it to the feed. Rejection is correlated to conductivity using **Equation 1**.

$$R = 1 - C_p/C_f \tag{1}$$

2.3 Result and Discussion

2.3.1 Polymer Characterization

NMR was carried out after each step of the polymer synthesis to ensure each reaction went to completion and all impurities were removed before the next step. An overview of the entire synthesis is shown in **Figure 7**.

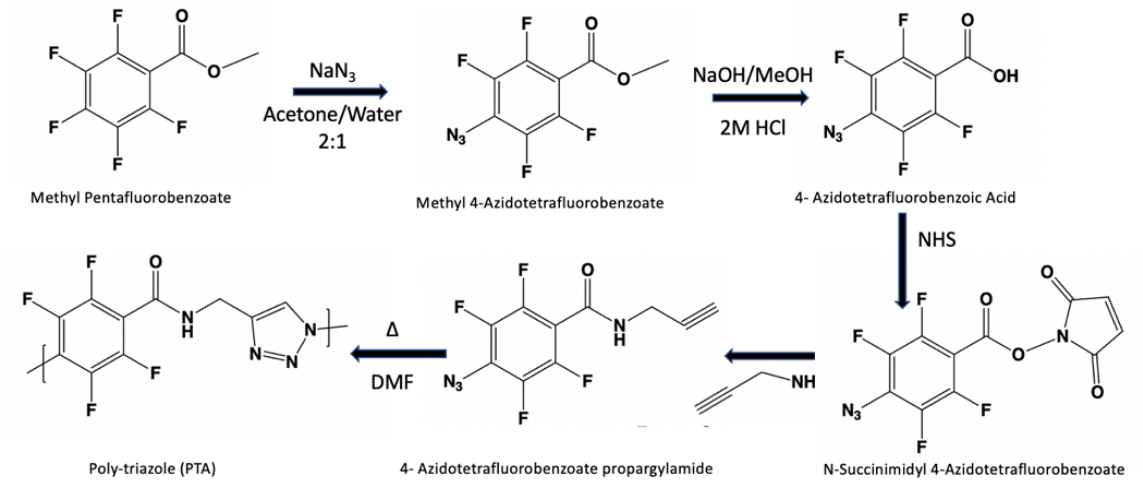

Figure 7: Poly-triazole synthesis schematic.

The first step in the synthesis was to add the azide onto the ring. Figure 8 shows the fluorine NMR between the benzoate before and after the azide is added. **Figure 8a** has 3 clear peaks representing the three distinctive fluorines in the molecules. Once the azide is added onto the para position, there are only 2 peaks left in **Figure 8b**. The smaller peaks that can also be seen are due to approximately 5% ortho addition.

The proton NMR of N-succinimidyl 4-azidotetrafluorobenzoate is shown in **Figure 9a**. The peak at 2.91 ppm is labeled on the molecule. For this NMR, I was

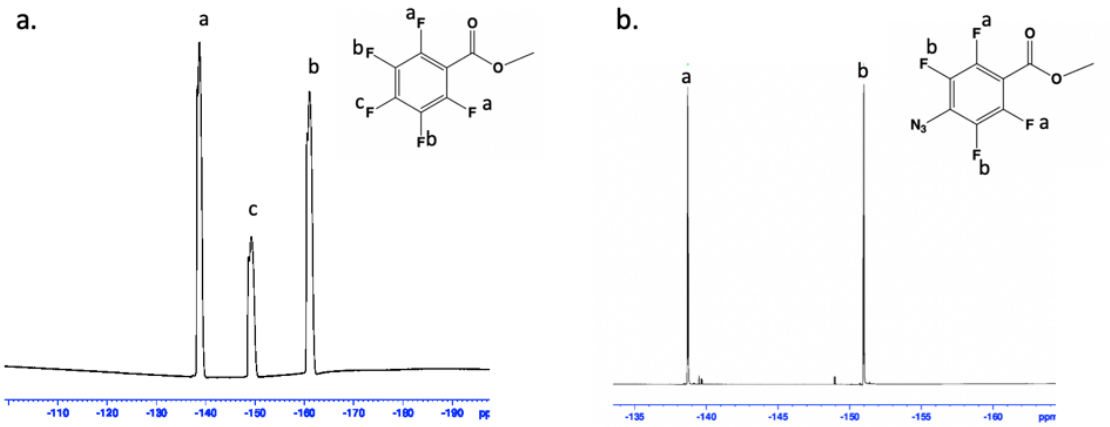

Figure 8: NMR before (a) and after (b) the azide was added.

primarily ensuring that any leftover DCC and NHS was removed after recrystallization. Unfortunately, there are still a few impurities from the DCC that can be seen between 1-2 ppm. These impurities are completely removed after the final polymer is purified.

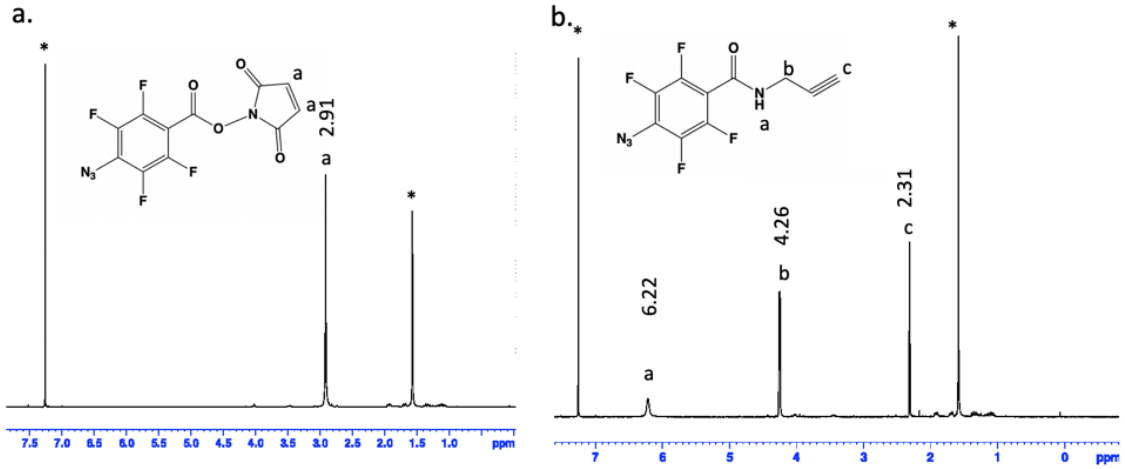

Figure 9: NMR of (a) the n-succinimidyl 4-azidotetrafluorobenzoate and (b) the 4-azidotetrafluorobenzoate propargylamide. Solvent peaks are marked with *.

The final step in creating the monomer, 4- azidotetrafluorobenzoate propargylamide, was accomplished by adding the propargylamine to the precursor in equal molar amounts. The propargylamine easily replaces the succinimidyl group leaving 3 NMR peaks as labeled in **Figure 9b**. The peak at 4.26 ppm had an integration twice that of the peak at 2.31 ppm confirming it belongs to the carbon with two protons.

The actual polymerization was very simple, using only heat. In addition to NMR, IR was also used in order to confirm the absence of the azide. Figure 11a is the NMR in deuterated DMSO. The polymer ideally will have three peaks that are all visible and labeled in the NMR. The aromatic peaks from the triazole that are all downfield are extremely small, as they tend to not absorb well. The amide peak (a) is at 8.28 ppm and the triazole proton peak is at 8.57 ppm. The third unlabeled peak at 7.91 ppm is possibly due to the slight amount of 1,5-disubstituted triazoles that account for around 10% of the reaction. The largest peak in the NMR comes from the one carbon chain at 3.30 ppm. **Figure 10b** was used to confirm the disappearance of the azide during the polymerization showing that the reaction goes to completion. Azides are typically seen from 2100-2270 cm^{-1} and this peak is large in the monomer. After the first day, IR spectra was taken and confirmed the azide peak lessons, however, it isnt until a second day of the reaction that the azide peak disappears almost completely which shows that the polymerization is very efficient.

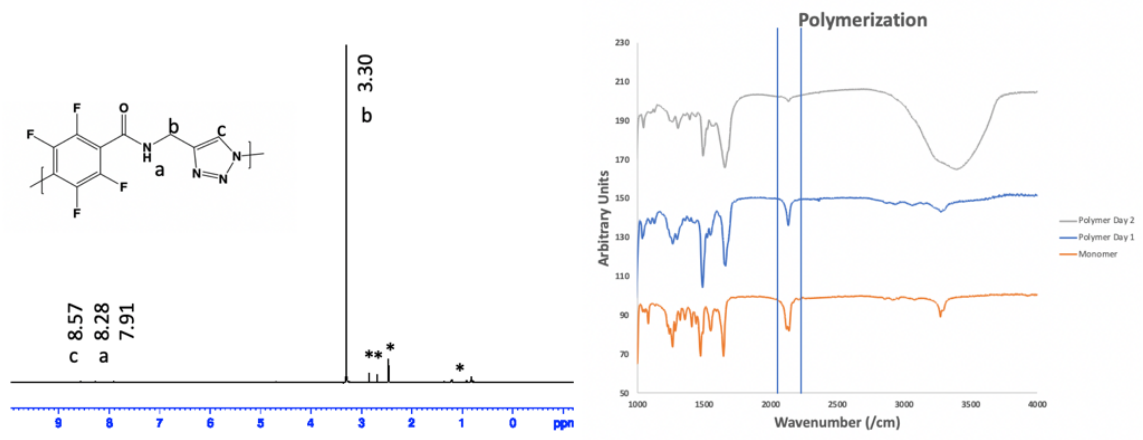

Figure 10: Left: NMR of PTA after 2 days of heating. Solvent peaks are labeled with *. Right: IR that shows the progression of the azide peak after heating at different time points.

2.3.2 Membrane Characterization

Once the polymer was synthesized it was fabricated into a reverse osmosis membrane. The PTA membrane was created by dissolving PTA in DMF at 15 mg/mL and casting it on a glass substrate. The epoxy support was poured over the active layer and pulled off using the T-FLO method. XPS was carried out on the membrane and is shown in **Figure 11a**. The XPS spectrum indicates covalent bonding between the epoxy and the PTA due to the increase in the N 1s peak. We believe that the cause of this is due to a ring opening reaction between the epoxide and the amide group on the PTA. Another indication is the presence of the F 1s peak, which is also visible in the XPS spectra. This is another clear sign that the active layer is on the support. **Figure 11b** is a picture taken after T-FLO. On the left we can clearly see the active layer, which is thin and shiny while the support, on the right is duller.

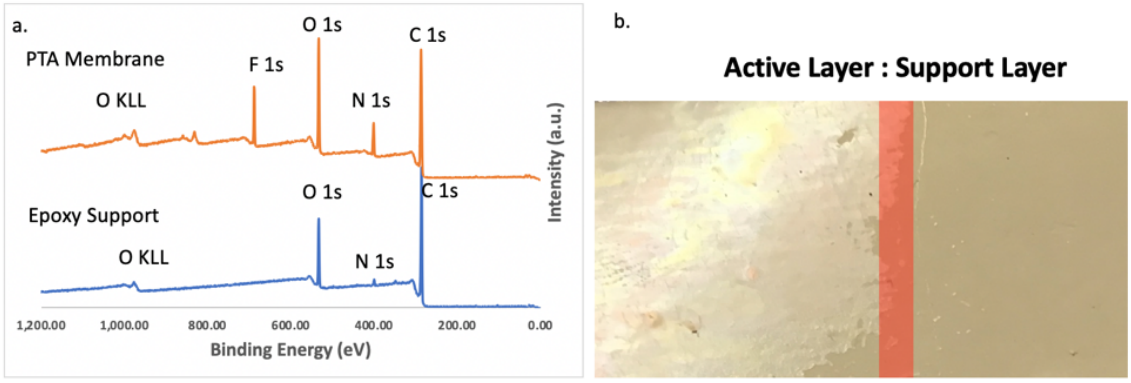

Figure 11: (a) XPS of the control epoxy support in comparison to the fabricated membrane with the PTA active layer. (b) Photo of the acitve layer on the left and support on the right.

2.3.3 Salt Rejection

Once the polymer was confirmed to bind to the epoxy, salt rejection testing was carried out to demonstrate that the PTA membrane can be successfully used for desalination. We created a PBI-PTA membrane blend, increasing the mechanical strength of the membrane with PBI. PBI is also known to not reject salt as it is not crosslinked and so it will swell, expanding the polymer. PBI also is not charged and so there are no ions to repel the salt. The support layer was optimized by using a blend of PEG-400 and PEG-200 to minimize compaction. 5 cm membrane coupons were punched out of the flat sheets and used for the rejection testing in a dead end cell apparatus. The conditions of the experiment were 10,000 ppm NaCl and the cell was operated at 800 psi. Rejection for both the control PBI, and the PBI-PTA blend are shown in Figure 13. The rejection the PBI/ PTA membrane achieved was 90%. The PBI membrane, however, only had 75% salt rejection.

2.4 Conclusion

In these sets of experiments we successfully synthesized a novel polymer, PTA, using click chemistry for membrane desalination. NMR and IR spectroscopy was used to confirm the successful synthesis of the polymer. A reverse osmosis membrane was created using PTA as the active layer on a porous epoxy support. The membranes were tested for salt rejection and we found that the membrane with the PTA polymer performed better than the PBI control. In the future, more membranes with varying amounts of PTA will be cast in order to correlate the salt rejection with the presence of PTA. Because this polymer was synthesized with chlorine tolerance in mind, chlorine tolerance experiments also need to be performed. Finally to improve the permeability, we would like to incorporate a different fabric support, such as carbon fiber, as it has larger pores and should facilitate better water permeability.

2.5 References

1. R. Matz, U. Fisher, *Desalination.* **1981**, 36, 137-141.

2. C.E. Reid, E.J. Breton, *J. Appl. Polym. Sci..* **1959**, 1, 133-143.

3. S. Loeb, *ACS Symposium Series.* **1981**, 153.

4. J. Glater, S. Hong, M. Elimelech, *Desalination.***1994**, 95, 325-345.

5. K.J. Edgar, C.M. Buchanan, J.S. Debenham, P.A. Rundquist, B.D. Seiler, M.C. Shelton, D. Tindall, *Prog. Polym. Sci..* **2001**, 21, 1605-1688.

6. H. Strathmann, A.S. Michaels, *Desalination.* **1977**, 21, 195-202.

7. S.H. Son, J. Jegal, *J. Appl. Polym. Sci..* **2011**, 120, 1245-1252.

8. J. M. Gohil, A. K. Suresh, *J. Mem. Sci..* **2017**, 531, 108-126.

9. Y. Liu, W. Zhao, C.H. Chen, A.H. Flood, *Science.* **2019**.

10. Y. Li, A. H. Flood, *Angewandte.* **2008**, 47, 2649-2652

11. C. L. D. Gibb, E. D. Stevens, B. C. Gibb, *J. Am. Chem. Soc..* **2001**, 123, 5849-5850.

12. H.C. Kolb, M.G. Finn, K. B. Sharpless, *Angewandte.* **2001**, 40, 2004- 2021.

13. V. V. Rostovtsev, L. G. Green, V. V. Folkin, K. B. Sharpless, *Angewandte.* **2002**, 41, 2596-2599.

14. Q. Wang, H. Li, Q. Wei, J. Z. Sun, J. Wang, X. A. Zhang, A. Qin, B. Z. Tang, *Polym. Chem.*. **2013**, 4, 13961401

15. L. HongKun, M. Ju , W. Jian , Z. Shuang , Z. QiuLi , W. Qiang , Q. AnJun1, S. JingZhi, T. B. Zhong, *Sci. China. Chem.*. **2011**, 54, 611-616.

16. B. H. Jeoung, E. M. V. Hoek, Y. Yan, A. Subramani, X. Huang, G. Hurwitz, A. K. Ghosh, A. Jawor, *J. Mem. Sci.*. **2007**, 294, 1-7.

17. B. McVerry, M. Anderson, N. He, H. Kweon, C. Ji, S. Xue, E. Rao, C. Lee, C. Lin, D. Chen, D. Jun, G. Sant, R. B. Kaner, *Nano. Lett.*. **2019**, 19, 5036-5043